A METHOD FOR CONSTRUCTING URBAN EXTENT MAP FROM ALOS/PALSAR SATELLITE DATA

Koichiro ITABASHI*[a], Hiroyuki MIYAZAKI[b], Koki IWAO[c], Kazuki NAKAMURA[d], Masashi MATSUOKA[e] and Ryosuke SHIBASAKI[f]

[a] Graduate student, Institute of Industrial Science, The University of Tokyo, 4-6-1 Komaba, Meguro-ku, Tokyo 153-8505, Japan; Tel: +81-3-5452-6417;
E-mail: itabashi@iis.u-tokyo.ac.jp

[b] JSPS fellow, Center for Spatial Information Science, The University of Tokyo, 5-1-5 Kashiwanoha, Kashiwa, Chiba 277-8568, Japan; Tel: +81-4-7136-4307;
E-mail: heromiya@csis.u-tokyo.ac.jp

[c] Researcher, National Institute of Advanced Industrial Science and Technology, Central 2, Umezono 1-1-1, Tsukuba, Ibaraki 305-8568, Japan; Tel: +81-29-862-6710;
Email: iwao.koki@aist.go.jp

[d] Researcher, National Institute of Advanced Industrial Science and Technology, Central 2, Umezono 1-1-1, Tsukuba, Ibaraki 305-8568, Japan; Tel: +81-29-862-6710;
Email: nakamura-kazuki@aist.go.jp

[e] Researcher, National Institute of Advanced Industrial Science and Technology, Central 2, Umezono 1-1-1, Tsukuba, Ibaraki 305-8568, Japan; Tel: +81-29-862-6710;
Email: m.matsuoka@aist.go.jp

[f] Professor, Center for Spatial Information Science, The University of Tokyo, 5-1-5 Kashiwanoha, Kashiwa, Chiba 277-8568, Japan; Tel: +81-4-7136-4307;
E-mail: shiba@csis.u-tokyo.ac.jp

KEY WORDS: ALOS/PALSAR, microwave sensor, urban extent map, classification

ABSTRACT: Currently, global urban extent map of high accuracy and high resolution have been constructed mainly using optical sensor including ASTER/VNIR. However, there are some regions where urban areas are not correctly detected due to cloud cover and similar reflectance among land cover classes. To solve the problems, we used microwave sensor images of ALOS/PALSAR, which has an advantage in enabling observation in all weather conditions. This study aims at examining the possibility of using ALOS/PALSAR images as an alternative data resource for constructing urban extent map. Firstly, to determine useful ALOS/PALSAR observation mode, we examined how often ALOS/PALSAR images are taken in the regions for which an existing method using ASTER/VNIR images could not detect urban area correctly. Secondly, we collected ALOS/PALSAR satellite images, and examined effect of local-incident-angle-corrected images of ALOS/PALSAR taken by Fine Resolution Mode which can reduce distortion of pixel values due to local incident angle. We also performed unsupervised classifications on the ALOS/PALSAR and local-incident-angle-corrected images. Finally, we discussed ground truth datasets for image classification.

1. INTRODUCTION

The impacts of climate change are increasing in many regions of the world (IPCC, 2007). More and different types of data indicating status of socio-economics are needed at several geographical levels (United Nations, 2004). The size, scale, and form of cities will be critical concern (Laumann, 2005). However amount and quality of data and literature on observed changes is not well balanced with marked scarcity in developing countries (IPCC, 2007).

For that reason, global urban extent map in high accuracy and high resolution have been constructed using optical sensor images such as Terra's ASTER/VNIR (Miyazaki et al, 2009). However, in the mapping of urban area by optical sensor, cloud contaminated pixels are major obstacles against the accuracy of products especially for tropical zone. Also, in desert regions, such methods using optical sensor images had misclassified bare land and desert as urban area, and vice versa (Miyazaki et al, 2009). It is because bare land and desert have similar characteristic in surface reflectance to urban area.

To deal with the problems, we focused to utilizing the images of a microwave sensor, ALOS/PALSAR. Microwave sensor enables observation in all weather conditions without any restriction by cloud or rain (Remote Sensing Note, 1996). Also, considering differences in both back scatter coefficient of microwave sensor and surface reflectance of optical sensor between bare land and urban area, urban area may be successfully detected in desert regions. For that reason, ALOS/PALSAR has the possibility for detecting urban area on regions which are likely to be misclassified by classification using only ASTER/VNIR optical sensor images and for developing global urban extent map in high accuracy and high resolution.

2. OBJECTIVE

The main objective of this project is to improve accuracy of urban extent map especially in the regions for which an existing method using ASTER/VNIR images could not detect urban area correctly. This paper focuses on the possibility of using ALOS/PALSAR images to construct urban extent map. To discuss above issues, we examined 1) observation condition of ALOS/PALSAR, 2) effect of ALOS/PALSAR local-incident-angle corrected images, 3) effect of ALOS/PALSAR raster data for detecting urban area.

3. METHODOLOGY

3.1. ALOS/PALSAR

In this study, we used ALOS/PALSAR satellite images. PALSAR is one of the sensors on ALOS, which was launched by JAXA in 2006. PALSAR has five different observation modes: Fine Beam Singlepolarization (FBS), Fine Beam Dual polarization (FBD), Polarimetric mode (POL), ScanSAR mode, and Direct Transmission (DT) mode (Rosenqvist et al., 2007).

Earth Remote Sensing Data Analysis Center (ERSDAC) publicly provides observation coverage maps of each ALOS/PALSAR's observation mode (http://www.palsar.ersdac.or.jp/e/guide/pdf/worldcoverage091027.pdf). However, it does not present whether a city undetected by ASTER/VNIR have been observed by ALOS/PALSAR. For that reason, we had to examine how often ALOS/PALSAR images have been taken for each city of our interest. The observation modes which we checked were FBS, FBD, and POL with setting search period from January in 2006 to March in 2011. We selected 100 cities including the regions for which an existing method using ASTER/VNIR images could not detect urban area correctly (Figure 1).

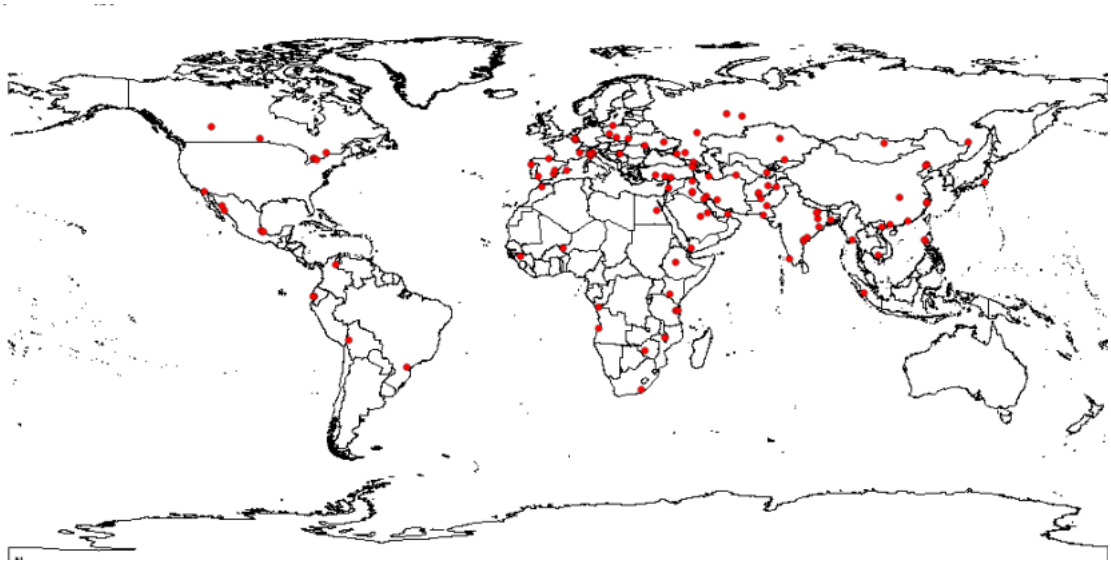

Figure 1. Location of the test cities. Red points represented the location of each city.

3.2. Local-incident-angle Corrected Images

3.2.1. Outline: In mountainous areas, pixel values of PALSAR images are often distorted due to high degree of local incident angle; therefore steep land might be misclassified as urban. To solve the problem, we performed a correction on ALOS/PALSAR images taken by Fine Resolution Mode with the following equations:

$$\gamma^0 = \sigma^0 / \cos\theta \quad (1)$$

$$\sigma^0{}_{cal} = \gamma^0 \times \alpha \quad (2)$$

where σ^0 is backscattering coefficient, θ is local incident angle, α is correction coefficient for local incidence angle. The orthorectified ALOS/PALSAR images were corrected based on local incident angle data calculated from ASTER GDEM.

3.2.2. Effect of Local-incident-angle Corrected Images: To examine the effect of local-incident-angle corrected images, we calculated difference of backscattering coefficient between original images and local-incident-angle corrected images using GRASS GIS software (version 6.4; http://wgrass.media.osaka-cu.ac.jp/grassh/). We calculated absolute value of difference between original pixel and local-incident-angle pixel values (Equation 3). In this paper, we term those two new maps as difference HH and difference HV. We chose two cities from mountainous areas as test sites. Those were La Paz, Bolibia, Mexicali, Mexico.

$$OutPixel = \left| InPixel_{inc\_ang\_cor} - InPixel_{original} \right| \quad (3)$$

where: $OutPixel_{difference}$ is calculated pixel value, $InPixel_{inc\_ang\_cor}$ is local-incident-angle pixel value, $InPixel_{original}$ is original pixel value.

3.2.3. Unsupervised Classification by Original and Local-incident-angle Corrected Images: We performed unsupervised classifications on the ALOS/PALSAR images using the ISODATA implemented by GRASS GIS software. To examine the effect of introducing the local-incident-angle correction, we had two cases of experiments: first, original HH and original HV (band set 1); second, original HH, original HV, local-incident-angle corrected HH, and local-incident-angle corrected HV (band set 2). We classified the images of two cities mentioned in section 3.2.2. After generating the clusters, we assigned urban class label to clusters by visual interpretation.

4. RESULTS

4.1. Observation Condition of ALOS/PALSAR

We counted how often ALOS/PALSAR images have been taken for 100 cities including the regions for which an existing method using ASTER/VNIR images could not detect urban area correctly. For the counting, we used product searching service operated by ERSDAC (https://ims1d.palsar.ersdac.or.jp/palsar_ims1_public/ims1/pub/en). To avoid counting overlapped scenes over paths, we counted images in a representative path for a city. As the result, we found that 6-10 FBS scenes and 6-11 FBD scenes per year were available for a city (Table 1). We also found that FBS and FBD have achieved yearly observation for every city of the 100 cities. On the contrary, POL has not been taken in some regions, for example, a part of China, Middle East, Central America, Central Asia, and Russia.

We conducted the classification on the cities for which the accuracy of the urban extent map derived from ASTER/VNIR (Miyazaki et al., 2009) were relatively low (Table 1). For every city, FBS and FBD were taken more than one time during the five years. For Matadi, Taizz, Rajahmundry, we could not find POL mode images. Therefore, we decided to use FBS and FBD mode as an alternative data resource for constructing the urban extent map. We also considered using POL images if available.

4.2. Difference Between Original and Local-incident-angle Corrected Images

Figure 2 and Figure 3 show the results of difference of backscattering between original image and local-incident-angle corrected image. The result shows that the differences in mountainous areas were larger than other areas, such as urban, forests and agriculture fields. It indicates that the backscatters in mountainous areas were successfully corrected by the local-incident-angle correction. We supposed that these characteristic differences might be useful to reduce misclassifications in mountainous areas.

4.3. Unsupervised Classification for Considering Effect of Local-incident-angle Corrected Images

Figure 4 and Figure 5 show the classification results of each city. Table 2 shows the area and the number of the pixel of the clusters assigned as urban. According to the Table 2, the size of the clusters assigned as urban is almost

same in all cases. It indicates that the number of bands might not have effected to improvement of classification accuracy.

We found that clusters assigned as urban tend to include mountainous areas (Figure 2, 3, 4, and 5). Therefore, introducing local-incident-angle correction would reduce such misclassifications and result in improvement of classification accuracy.

Table 1: Observation condition of ALOS/PALSAR on the cities for which accuracy of the urban extent map derived from ASTER/VNIR (Miyazaki et al., 2009) were relatively low

City	Country	Kappa coefficient of urban extent map derived from ASTER/VNIR images (Miyazaki et al., 2009)	FBS	FBD	POL
Curitiba	Brazil	0.052747	8	11	2
Guayaquil	Ecuador	0.001769	7	10	3
Matadi	Democratic Republic of the Congo	0.039023	8	9	-
Taizz	Yemen	0.02004	10	9	-
Lviv	Ukraina	0.044101	10	8	1
Chisinau	Moldova	0.090227	7	8	4
Palma	Spain	0.0035471	9	9	3
Xalapa	Mexico	0.004578	6	6	2
Rajahmundry	India	0.006139	6	6	-
Vijayawada	India	0.001191	9	11	4
Peshawar	Pakistan	0.081779	6	7	2

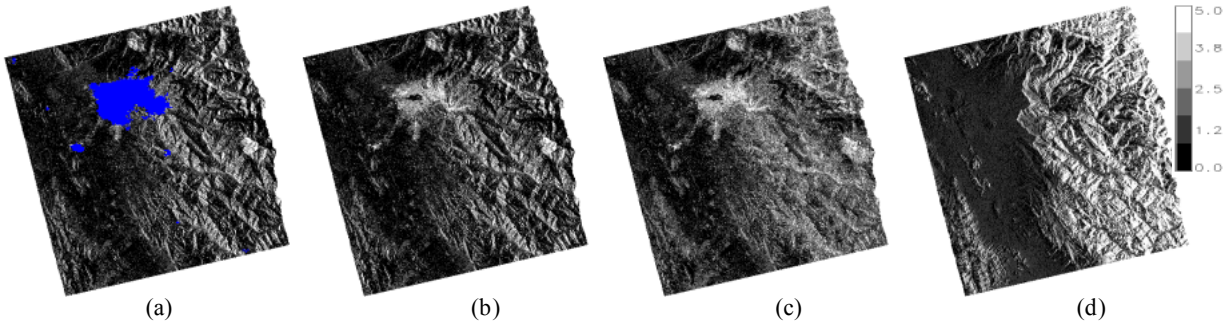

(a) (b) (c) (d)

Figure 2. Effect of local-incident-angle corrected images in La Paz, Bolibia (-68.16, -16.50). (a) Urban area maps derived from MCD12Q1 (blue pixel) (b) original HH (c) local-incident-angle corrected HH (d) difference of backscattering coefficient between (b) and (c).

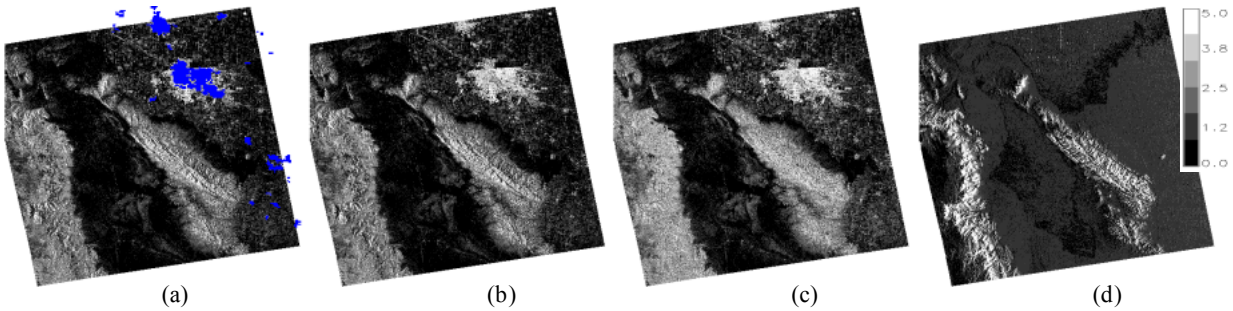

(a) (b) (c) (d)

Figure 3. Effect of local-incident-angle corrected images in Mexicali, Mexico (-115.46, 32.65). (a) Urban area maps derived from MCD12Q1 (blue pixel) (b) original HH (c) local-incident-angle corrected HH (d) difference of backscattering coefficient between (b) and (c).

Table 2: Area and pixel count of clusters including urban areas in La Paz and Mexicali.
band set 1: original HH and original HV, band set 2: original HH, original HV, local-incident-angle corrected HH, and local-incident-angle corrected HV

City	Country	Input bands	Area (km2)	Number of pixels
La Paz	Bolivia	band set 1	962.51	4225595
		band set 2	907.82	3985486
Mexicali	Mexico	band set 1	1059.36	5264040
		band set 2	1077.34	5353388

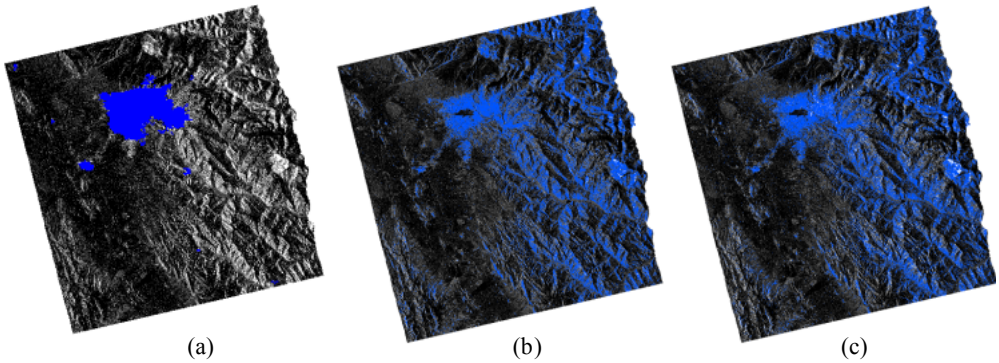

(a) (b) (c)

Figure 4: Classification results for La Paz, Bolibia (-68.16, -16.50). (a) Urban area maps derived from MCD12Q1 (b) input band is band set 1 (c) input band is band set 2. Blue pixel represents urban area. Back ground images are original HH.

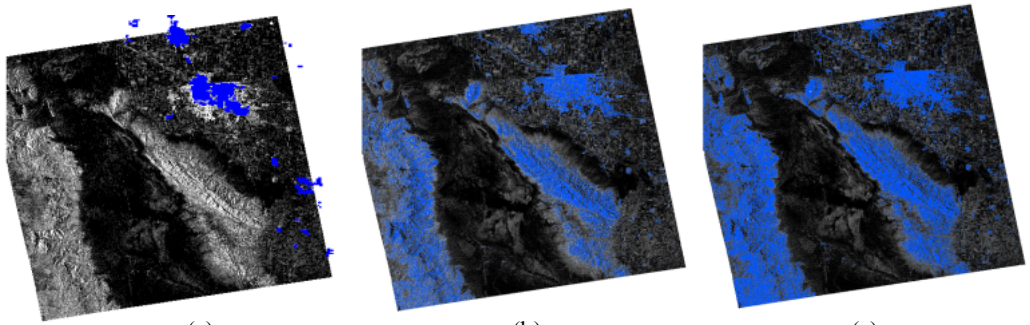

(a) (b) (c)

Figure 5: Classification results for Mexicali, Mexico (-115.46, 32.65). (a) Urban area maps derived from MCD12Q1 (b) input band is band set 1 (c) input band is band set 2. Blue pixel represents urban area. Back ground images are original HH.

5. DISCUSSION

5.1. Ground Truth Data for Image Processing

In Miyazaki et al. (2011), they developed a new ground truth database for urban areas from GRUMP Settlement Points. However, it is not enough to utilize this database as both training data and validation data because there are about only a few points (urban or non-urban points) for a scene. If we use these point datasets as training data and validation data, it is necessary to increase ground truth datasets.

5.2. Using Road Maps as Ground Truth Datasets

Urban extent map derived from ASTER/VNIR images (Miyazaki et al., 2009) had employed existing coarse-resolution global urban maps as training data, such as urban and built-up area class of MCD12Q1 (Center for Earth Resource Observation and Science, 2009). Though MCD12Q1 urban and built-up map has been evaluated as the most accurate map (Potere et al., 2009), misclassification might be occurred in the regions where MCD12Q1 does not classify urban areas correctly. For that reason, we consider to utilize road network data from Open Street

Map (OSM) (http://www.openstreetmap.org/) as additional ground truth datasets. Figure 6 shows an example of OSM in Dubai, UAE. OSM cover urban area where urban map from ASTER/VNIR and MCD12Q1 could not detect (south-west of the city). Therefore OSM data might be an alternative training datasets.

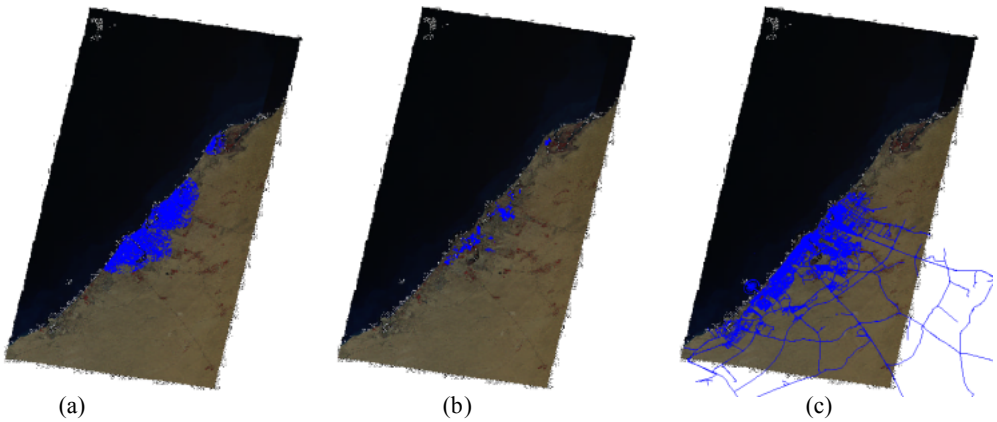

(a) (b) (c)

Figure 6. (a) urban area map derived from ASTER/VNIR (b) urban area map derived from MCD12Q1 (c) road network map from OSM. Blue pixels in (a) and (b) represents urban area. Blue lines in (c) represents road. Back ground images are false-color composite image of ASTER/VNIR.

6. CONCLUTIONS

We examined possibility of using ALOS/PALSAR images to construct urban extent map. As the result, we decided to use FBS and FBD mode as an alternative data resource for constructing the urban extent map. We also considered using POL images if available. We also found that clusters assigned as urban tend to include mountainous areas. Therefore, introducing local-incident-angle correction would reduce such misclassifications and result in improvement of classification accuracy. For future works, we will implement and experiment the classification method with statistical theory and machine learning theory for more accurate detection of urban area, and develop a new ground truth dataset from road maps.

ACKNOWLEDGEMENT

This research used PALSAR Data beta and ASTER Data beta processed by the AIST GEO Grid from PALSAR Data owned by METI and JAXA and ASTER Data owned by METI.

REFERENCE

IPCC, 2007. Summary for Policymakers. In : Climate Change 2007 : Impacts, Adaptation and Vulnerability. Contribution of Working Group II to the Fourth Assessment Report of the Intergovernment Panel on Climate Change, pp.7-22.

United Nations, 2004. Agenda21, 28th April 2009, http://www.un.org/esa/sustdev/documents/agenda21/index.htm

Laumann, G., 2005. Science Plan: Urbanization and Global Environmental Change, IHDP Report Series No. 15, International Human Dimensions Programme on Global Environmental Change, 61pp.

Miyazaki, H., Tanaka, A., Iwao, K., and Shibasaki, R., 2009. A Method for Developing Urban Extent Map of High Accuracy and Resolution by Integrating ASTER/VNIR Images and Existing Urban Extent Maps. Journal of the Japan society of photogrammetry and remote sensing. 48(2), pp.82-96.

Japan Association on Remote Sensing, 1996. Remote Sensing Note. 2nd issue.

Rosenqvist, A., Shimada, M., Ito, N., Watanabe, M., 2007. ALOS PALSAR: A Pathfinder Mission for Global-Scale Monitoring of the Environment. IEEE Transaction on Geoscience and Remote sensing, 45(11), pp.3307-3316.

Miyazaki, Hiroyuki; Iwao, Koki; Shibasaki, Ryosuke. 2011. "Development of a New Ground Truth Database for Global Urban Area Mapping from a Gazetteer."Remote Sens. 3, no. 6: 1177-1187.

Potere, D., A. Schneider, S. Angel, and D. L. Civco 2009. “Mapping urban areas on a global scale: which of the eight maps now available is more accurate?”. International Journal of Remote Sensing, 30(24) pp.6531–6558.